TWEET-IE
Twin Wind tunnels for Energy & the EnvironmenT
INNOVATIONS - EXCELLENCE

Twin Test Results

Authors: V. Pappa, K. Kellaris, G. Chondromatidis, N.-P. Pallas, B. DSouza, L. Calzoni , S. Tamaro, J. Prospathopoulos, P. Chasapogiannis, , F. Campagnolo, F. Muhle, C. Gromke, A. Sciacchitano, A. Croce, C. Bottasso, M. Manolesos, V. Riziotis, D. Bouris

Lead Beneficiary: NTUA

Dissemination Level: PU-Public

Deliverable 3.1

WP3

TWIN TESTS

TWEET-IE / Twin Wind tunnels for Energy and the EnvironmenT - Innovations and Excellence
HORIZON-WIDERA-2021-ACCESS-03-01 / PR# 101079125

Co-funded by the European Union

HISTORY AND CHANGES

Ver	Date	Description	Contributors
00	28/08/2025	Report	NTUA

Co-funded by the European Union

TABLE OF CONTENTS

1 Executive Summary 3
2 Twin Test 1: Effects of Vegetation on Flows in the Urban Environment 5
2.1 Background & Introduction 5
2.2 TWT Setups 5
2.3 Results & Discussion 10
2.4 Conclusions 15
3 Twin Test 2: Wake Interactions of a Cluster of Turbines and Wake Steering Techniques 16
3.1 Introduction 16
3.2 Experiment description 16
3.3 Results 17
3.4 Additional Wind Tunnel Tests 19
3.5 Conclusions 20
4 Twin Test 3: Micro devices for Enhanced Performance of Airfoil Sections 21
4.1 Background & Introduction 21
4.2 TWT Setups 21
4.3 Results & Discussion 23
4.4 Conclusions 25
5 Twin Test 4: Scale Effects in Urban Flows 26
5.1 Introduction 26
5.2 Experiment description 26
5.3 Test Matrix 28
5.4 Results 29
5.5 Additional Wind Tunnel Tests 31
5.6 Conclusions 32
6 Publications 33
7 References 35

Co-funded by the European Union

1 Executive Summary

This deliverable sums up the research component of TWEET-IE, corresponding to pillar II: Widening of technical capacity and competence via the Twin Tests (Twin Tests - TWTs) and benchmarking campaigns. The results of the TWTs address the main research challenge i.e. to identify, characterize, categorize and then restrain important sources (external conditions, testing equipment etc.) of deviations between test data obtained at different wind tunnels. NTUA WT capabilities are compared to the state of the art and particularities have been defined. Each of the four TWTs comprises at least two WT test campaigns of identical test matrices: one at NTUA and the other at one of the Leading Partners. Both tests are conducted by NTUA scientific and technical personnel under the guidance and supervision of specialized personnel of the corresponding Leading Partner. Technical competence for the TWT but also for future activities and NTUA research profile enhancement, was achieved through training activities (considered separately as part of WP4). The four TWTs, with the minor modifications agreed upon during the kick off meeting, are summarized below.

TWT1 Twin Tests on the effects of vegetation on flows in the urban environment. (NTUA, KIT). Airflow measurements were carried out using stereo PIV on several planes in and around a generic building exposed to an urban atmospheric boundary layer. Vegetation was on the building's external surfaces (upstream façade or rooftop). Tests were performed at the KIT and NTUA WTs where upstream atmospheric boundary layer (ABL) conditions were simulated, processed and evaluated (VDI 3783/12 standard). The scale for the buildings and flow was ~1:250-300. WT tests and measurements have been supported and complemented by CFD calculations performed by NTUA and international partners with in-house and/or open-source software.

TWT2 Twin Tests on wake interactions of a cluster of turbines and wake steering techniques. (NTUA, TUM). Performance measurements and flow field measurements in the wakes of a cluster of 0.6m diameter turbines resembling a wind farm configuration were carried out. The model turbines (owned by TUM) have integrated torque, pitch (cyclic) and yaw control capabilities. Wake flow measurements were conducted in the low speed section of NTUA WT and in the atmospheric tunnel of TUM using PIV and hot wire anemometry. Wake deflection (skew angle) in different yaw and tilt misalignment conditions were assessed through wake flow measurements for the cluster of turbines operating in misaligned inflow conditions. WT tests were supported by CFD aerodynamic simulations of the tested configurations, performed by NTUA and international partners using in-house and open source tools.

TWT3 Twin Tests on micro devices for enhanced performance of airfoil sections. (NTUA, POLIMI). Aerodynamic performance measurements and flow field measurements in the vicinity of a high aspect ratio wing (2D measurements) equipped with a) trailing edge micro tabs b) trailing edge Gurney flaps c) novel delta wind vortex generators. The TWT was conducted in the high speed (small) section of NTUA WT and in high speed (small section) of POLIMI WT. Steady-state measurements were performed for all devices (various fixed positions of the device and steady inflow conditions at various angles of attack). Exceptionally, imposed periodic motions of the Gurney flap were analyzed (relevant for load mitigation applications) and unsteady pressures on the section were recorded. PIV measurements were conducted

Co-funded by the European Union

in the vicinity of all devices. WT tests are supported by CFD aerodynamic simulations of the tested configurations that were performed by NTUA using in-house and open source tools.

TWT4 Twin Tests on scale effects in urban flows. (NTUA, TU Delft). Large scale PTV study of the flow past a simplified urban street canyon on which a smaller scale (vegetation) is introduced. Uniform upstream flow was used in order to limit the parameters being studied. Tests performed at TUDelft reached a Reynolds number double that of the scale studied in the NTUA WT ($Re \approx 10^5$ vs $Re \approx 5\ 10^4$, respectively). A robotic arm PTV system was transported to NTUA, ensuring comparable resolution and uncertainties. Universality of WT measurements and scale effects were documented in the characteristics of the flow such as in-canyon vortex position, reattachment on the building roof and pressure distribution on the canyon walls. Vegetation was modeled with appropriate pre-fabricated material and placed on the building roofs (rooftop greening) and on the canyon floor (hedge rows), drawing on the expertise of KIT.

Results of the twin tests have already been made publicly available on the zenodo platform, abiding by FAIR principles.

Co-funded by the European Union

2 Twin Test 1: Effects of Vegetation on Flows in the Urban Environment

2.1 Background & Introduction

In the context of studying vegetation effects on flow in the urban environment, twin tests of the flow past a cube shaped building were performed in the wind tunnels of the Karlsruhe Institute of Technology (KIT) and the National Technical University of Athens (NTUA). Identically shaped buildings with openings were used with comparable upstream atmospheric boundary layer profiles in terms of mean velocity, turbulence intensity and integral length scales. Simulated vegetation was placed on the windward building wall and on the rooftop, to simulate vertical wall and rooftop greening. Measurements were performed with Laser Doppler Velocimetry (LDV) at KIT and Particle Image Velocimetry (PIV, 2D-3C) at NTUA. The two measurement sets indicate the same qualitative trends of flow structure and vegetation effects and quantitative results are in close agreement. Results are publicly available [1] and provide an opportunity to analyse the effects of differences in upstream conditions, wind tunnel configurations and measurement techniques.

2.2 TWT Setups

One of the main goals of the study was to achieve, as much as possible, identical experimental setups in the two wind tunnels. This involved the building model's geometry, the simulated vegetation, the upstream mean flow and turbulence characteristics and Reynolds number independence. The test sections upstream of the turntable in the wind tunnels at Karlsruhe Institute of Technology (KIT) and the National Technical University of Athens (NTUA) are shown in Figure 1. The tunnels' cross sections (width×height) are 2.0×1.0m at KIT and 3.5×2.5m at NTUA, both ensuring constant streamwise pressure (dp/dx=0).

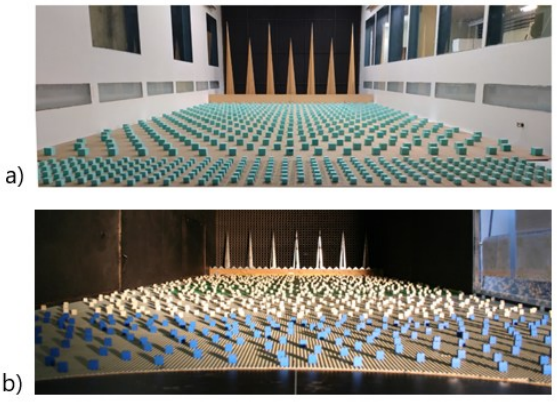

Figure 1. Atmospheric boundary layer (ABL) setups upstream of the turntable at a) NTUA test section and at b) KIT test section.

2.2.1 Comparison of ABL simulations

The upstream boundary layer profiles of mean streamwise velocity and turbulence intensity were measured with constant temperature hot wire anemometry (see Figure 2). The free stream velocity was U_∞=5 m/s in both wind tunnels but the reference velocity, taken at building height, was U_{ref}= 3.27 m/s at KIT and U_{ref} =2.36 m/s at NTUA, giving building height Reynolds numbers of Re_H=2.4 × 10^4 and 1.65× 10^4,

Co-funded by the European Union

respectively. Both of these values are above the commonly accepted Re independence limits of $Re \geq 10^4$ [2,3,4]. Vertical profiles of three main flow characteristics were determined: the mean velocity (Figure 2a), the turbulence intensity (Figure 2b) and the integral length scale (Figure 2c) in the streamwise direction. All figures include a zoom-in for non-dimensional heights, z/z_{ref} up to 2H, which were considered sufficient to show the variations and the differences of the calculated values. The comparison of the velocity measurements and the turbulence intensity calculations shows that the NTUA ABL configuration corresponds to a suburban terrain type, while KIT corresponds to an urban terrain type [5]. However, since the profiles correspond to the upper (suburban, NTUA) and lower (urban, KIT) boundaries of their characterization regions [5], they are actually quite close and may be considered comparable, at least up to two building heights from the ground. Indeed, the maximum differences of the mean velocity profiles are <3% while the corresponding differences between the turbulence intensity profiles are <7%. When comparing the turbulence integral length scale profiles, the average differences are ~28% and reach 50% at intermediate heights. The reason for these differences is presumed to be related to the different size of the test sections in the two wind tunnels (~ 1:4). These differences are noted but, given the mean velocity and turbulence intensity profiles, the results are considered favourable for comparing the measurements in the two wind tunnels and the measurements of the flow past the same model building provide valuable insights through the cross-comparison.

2.2.2 The model building

The aim of the experiments performed in both atmospheric boundary layer wind tunnels was to capture the flow field around and along the apertures of a model building when the greening is implanted either on the windward building wall or on the building's rooftop.

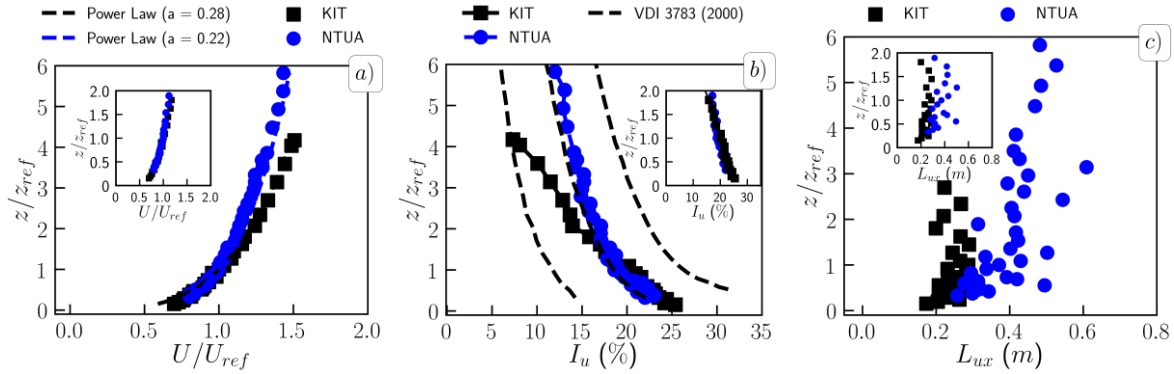

Figure 2. a) Non dimensional wind speed, U/U_{ref} , b) turbulence intensity, I_u and c) integral turbulence length scale, L_{ux} (in m) as a function of the height (z/z_{ref}) from the wind tunnel floor (z_{ref} = 110 mm) for the upstream profiles measured at KIT (black squares) and NTUA (blue dots).

In order to measure the flow field at the openings (KIT), it was necessary to simultaneously seed inside and outside the model building. For this reason, a special construction on the model building floor was considered, as this represents the area seeding source release. To facilitate optical access for the LDV measurements, the material of the cube had to be transparent to light in the visible wavelength range. Therefore, a new model building made of glass (see Figure 3a) with a layer thickness of 5 mm was constructed since Plexiglas is much more susceptible to surface scratches than glass. The height of the

Co-funded by the European Union

building model was H=110 mm, and the vertical openings on its side were: (height), h_e = 90 mm and (width), w_e = 6 mm. Inside the building, at the center, there was a vertical column of square cross section (22x22 mm). For the PIV measurements at the NTUA test section, the same model building was used as in [6]. The choice of settings and model buildings was made with emphasis on the geometric, dynamic and kinematic similarities in both wind tunnel setups. It served the purpose of compatibility with previous pressure measurements [6], comparison with previous PIV measurements performed at the NTUA test section and of comparison with the LDV measurements. An illustration of the Plexiglas model building can be found in Figure 3b.

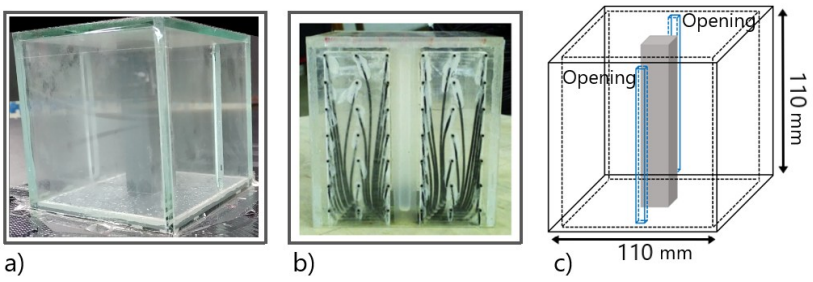

Figure 3 The model building with the two side wall parallel apertures made of glass and used in LDV experiments at KIT, b) the plexiglass model building used in PIV experiments at NTUA and c) a simple sketch of the hollow model building with dimensions (in mm)

2.2.3 Vegetation model characterization and investigated cases

The modeling of vegetation in wind tunnel studies was described and analysed in detail in [6], where the artificial material, i.e. propylene porous foam, was selected to simulate the properties of the vegetation, including the pressure loss coefficient, λ, the Leaf Area Density, *LAD*, the porosity, ε, the geometric properties such as thickness, *T*, and the product of $\lambda \cdot T$, which corresponds to the momentum absorption of the vegetation. All these vegetation properties were calculated both at reduced scale and at full scale, by applying the similarity laws and considering the corresponding scale factors of each wind tunnel, i.e. M_{NTUA} = 1:252 and M_{KIT} = 1:300. Due to the different scale factors, the corresponding values of the vegetation parameters in full scale differ in both wind tunnels, but these differences remain within the same limits, with negligible effect on the interpretation of the results. A summary of the vegetation parameters calculated in both wind tunnels is presented in Table 1. The cyan-coloured cells of the table correspond to the vegetation cases that were investigated in the NTUA wind tunnel using the PIV method for both greening positions, i.e. windward façade greening and rooftop greening. The green coloured cells represent the vegetation cases that were investigated in the KIT wind tunnel using LDV measurements. Based on this, three common vegetation scenarios were selected for the comparisons.

Co-funded by the European Union

Table 1. Summary of the comparison of the experimental results of the tested foam material for modeling vegetation parameters at NTUA and KIT, with different scale factors, *M*, pores per inch of foam samples (PPI), porosity, ϵ (%), foam thickness at reduced scale, T_{rs} (mm), and at full scale, T_{fs} (m), pressure loss coefficients at reduced scale, λ_{rs} (m^{-1}), and at full scale, λ_{fs} (m^{-1}), the product of pressure loss coefficients and the corresponding thickness at full scale, λT(-), and leaf area densities at full scale, LAD_{fs} (m^2 m^{-3}).

Wind tunnel *M*, Scale factor	Foam (pores per inch)	Porosity, ϵ (%)	T_{rs} (mm), T_{fs} (m)	λ_{rs} (m^{-1})	λ_{fs} (m^{-1})	$\lambda \cdot T$ (-)	LAD_{fs} (m^2 m^{-3})
NTUA	PPI60	96.58 ± 0.11*	10 mm / 2.5 m	2346	9.31	23.5	31
M_{NTUA} = 1 : 252	PPI30	97.15 ± 0.10*	10 mm / 2.5 m	1000	3.97	10.0	13.2
	PPI20	97.30 ± 0.12*	10 mm / 2.5 m	500	1.98	5.0	6.6
	PPI10	97.55 ± 0.15*	10 mm / 2.5 m	250	0.99	2.5	3.3
	PPI30	97.15 ± 0.10	5 mm / 1.3 m	913	3.62	4.6	12.1
	PPI20	97.30 ± 0.12	5 mm / 1.3 m	468	1.86	2.3	6.2
	PPI10	97.55 ± 0.15	5 mm / 1.3 m	194	0.77	1.0	2.6
KIT	PPI60	96.58 ± 0.11*	10 mm / 3.0 m	2346	7.82	23.5	26.1
M_{KIT} = 1 : 300	PPI30	97.15 ± 0.10*	10 mm / 3.0 m	1000	3.33	10.0	11.1
	PPI20	97.30 ± 0.12*	10 mm / 3.0 m	500	1.67	5.0	5.6
	PPI10	97.55 ± 0.15*	10 mm / 3.0 m	250	0.83	2.5	2.8
	PPI30	97.15 ± 0.10	5 mm / 1.5 m	913	3.04	4.6	10.1
	PPI20	97.30 ± 0.12	5 mm / 1.5 m	468	1.56	2.3	5.2
	PPI10	97.55 ± 0.15	5 mm / 1.5 m	194	0.65	1.0	2.2

* indicates values measured for same material at different thickness

2.2.4 Measurement Setup

Measurements were performed for several experimental configurations (see Table 2) at locations on the side, the roof, the wake of the building and along the openings of the model building. The measurements at KIT were performed with 2 component Laser Doppler Anemometry (LDA, 2D-2C) at three sampling frequencies of 100, 250 & 500Hz : i) along three vertical profiles on the roof and three vertical profiles in the wake, ii) along three horizontal profiles on the side wall of the model building including the measurement locations upstream and downstream of the side opening and iii) along the side opening, at various vertical positions. At NTUA, Stereo Particle Image Velocimetry (2D-3C, Stereo PIV) was employed on the roof - wake - side parallel planes, while Mono PIV (2D-2C) was adopted for the side horizontal plane, (perpendicular to the building's side wall). Schematics of both experimental set ups and their measurement locations can be found in Figure 4a-b.

Co-funded by the European Union

Table 2. Experimental configurations for which velocity measurements were acquired on the PIV measurement planes (NTUA) and on the LDV measurement positions (KIT).

Bare Building (No Open.) ∇	Bare Building (Two Open.) △	Façade greening □	Rooftop greening ○				
Inflow (0°)	PIV planes			LDV positions			
Vegetation cases	Side (Horiz./Paral.) *	Roof	Wake	Side	Roof	Wake	Openings
Bare Building (No Open.)	∇ / ∇	∇	∇	No	No	No	No
Bare Building (Two Open.)	△ / △	△	△	△	△	△	△
PPI60 (10 mm)	□ / ○	□ / ○	□ / ○	□ / ○	□ / ○	□ / ○	□ / ○
PPI30 (10 mm)	No / No	No	No	□ / No	□ / No	□ / No	□ / ○
PPI20 (10 mm)	□ / ○	□ / ○	□ / ○	□ / No	□ / No	□ / ○	□ / ○
PPI10 (10 mm)	No / No	No	No	No	No	No	□ / ○
PPI30 (5 mm)	No / No	No	No	No / ○	No / ○	No / ○	□ / ○
PPI20 (5 mm)	□ / ○	□ / ○	□ / ○	□ / ○	□ / ○	□ / ○	□ / ○
PPI10 (5 mm)	No / No	No	No	No	No	No	□ / ○

* indicates Side Horizontal & Side Parallel planes.

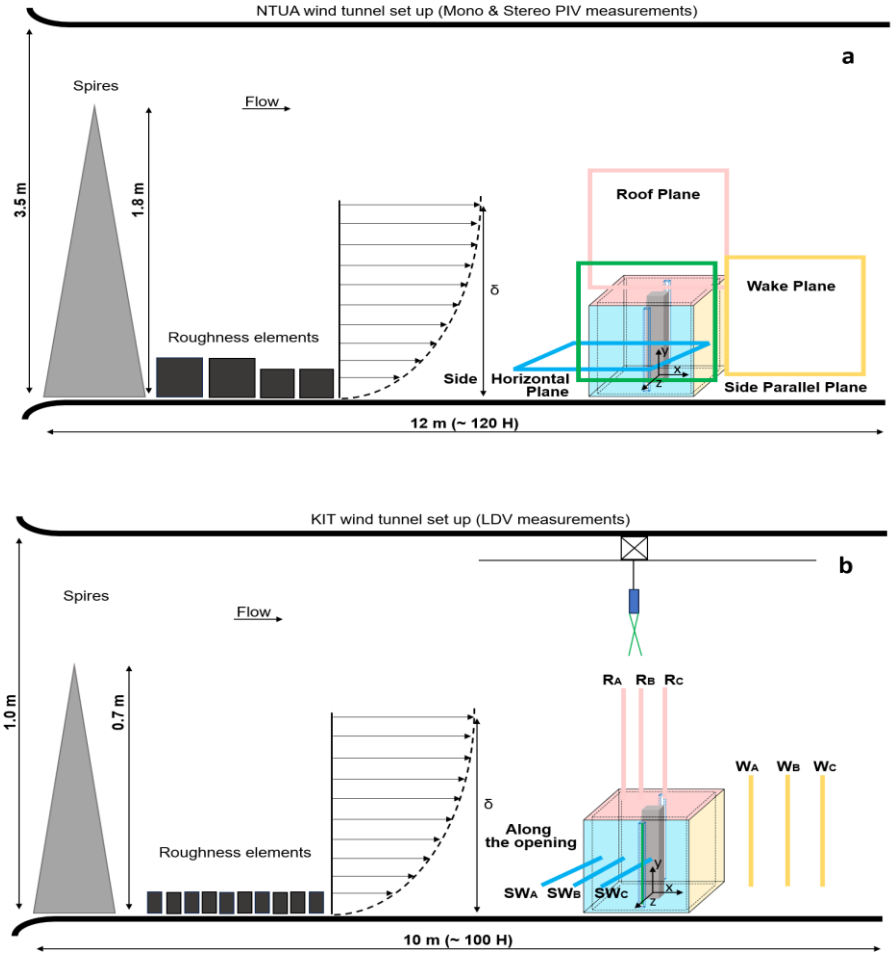

Figure 4. a) Schematic of the experimental setup of the model building with side wall apertures, as tested in the ABL wind tunnel facility at NTUA, presenting the PIV (Mono and/or Stereo) measurement planes : i) on the roof (pink SPIV) ii) on the side wall (blue MPIV), iii) in the wake (yellow SPIV) and iv) on the side (parallel to flow) wall (green SPIV) and b) the same experimental set up at KIT, presenting the LDV measurement locations : i) on the roof (R_A, R_B, R_C), ii) on the side wall (SW_A, SW_B, SW_C, iii) in the wake (W_A, W_B, W_C) and iv) along the vertical opening.

Co-funded by the European Union

2.3 Results & Discussion

This section presents the results of the velocity measurements around and through the openings of a cubic model building without/with two side openings, in combination with implanted greening on its surface walls, measured in the NTUA and KIT wind tunnels. Due to the large amount of data and for the convenience of the reader, the following format was chosen to present the results: at the beginning an indicative comparison of the model building results (with two side openings) at the common measurement locations, showing a comparison of the applied measurement technique (PIV, LDV), then the illustration of the flow field around the cube through the variable contours and the flow lines including all tested configurations to assess the effect of the implanted greening and to quantify the measurement method. More details regarding the post processing of the experiment data can be found in [7].

2.3.1 Bare building with two side openings : roof case

The flow field measurements on the roof of a model building with two side wall openings can provide us with a revealing picture of the velocity distribution around the building's outer surfaces. Figure 5a-c and Figure 6a-c show the mean, $\overline{u}$ and the *rms*, $\overline{u_{rms}}$ streamwise velocity profiles acquired along the height, using either the PIV technique (black line, NTUA) or the LDV technique (white square, KIT) at the three measurement locations, i.e. R_A, R_B and R_C, defined in Figure 4 . The ordinate represents the dimensionless (wrt building height) distance above ground level. Exact coordinates of all measurement positions can be found in [7]. Figure 5a-c shows a qualitative agreement between the velocity results in the two wind tunnels but a quantitative difference is observed. In particular, it becomes clear that the LDV measurements show higher non-dimensional streamwise velocity values than the corresponding PIV results, far from the roof with a difference of ~20%. However, this is a result that was to be expected as these mean streamwise velocity differences had already been observed in the ABL inlet profiles. In particular, from Figure 2a at the corresponding heights (s/H = z/z_{ref} -1) the differences in the mean upstream velocity profile are <15%. Closer to the roof level, where the recirculation zone resulting from separation from the leading edge is expected, the differences are smaller (~ 8%). A parameter that we should mention during the interpretation of the results is the blockage effect. Specifically, despite the fact that the blockage $a_{blockage}$ is ≤ 1 % in both wind tunnels, one should take into account that the cubic building's height corresponds to 0.1 m/1 m = 10 % of KIT wind tunnel's height and 0.1 m/2.5 m = 4 % of NTUA wind tunnel's height. Turning into the plots of the *rms* streamwise values, $\overline{u_{rms}}$: far from the roof (s/H ≥ 1.3H) there is a good agreement between the two measurement sets (LDV and PIV results), while closer to the roof level, the differences are approximately ~ 50%. These differences can be attributed to the differences in the measured turbulence intensity, I_u, as observed in the inlet profiles, where the values in the KIT measurmenets were significantly higher compared to those of NTUA. It can be deduced that despite the non-dimensionalization of the mean velocity values and the good agreement of the upstream flow between the two wind tunnels, some discrepancies are observed. This may be attributed to the different measurement systems (technique and uncertainties) together with a potentially high sensitivity to even small differences in the different ABL upstream velocity and turbulence profiles. The extent to which one parameter influences the other is not clear as it was not possible to use the same measurement system or precisely the same ABL setup in the two wind tunnels.

Co-funded by the European Union

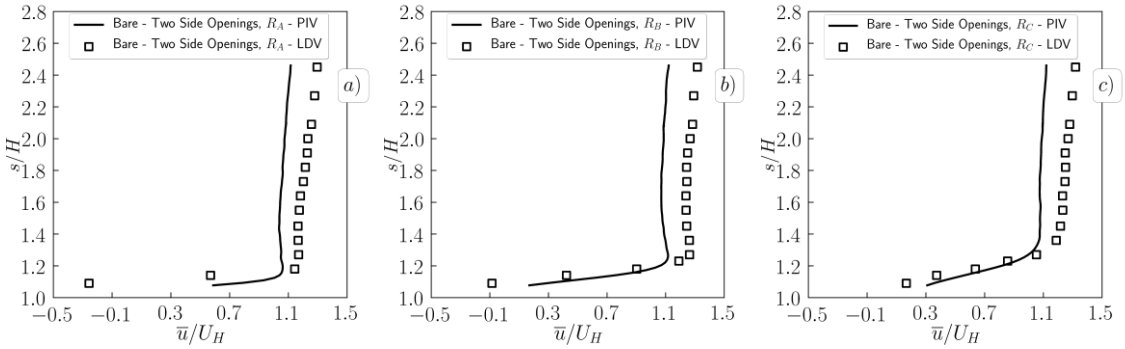

Figure 5. Comparison of the vertical profiles of the non-dimensional mean streamwise velocity component, $\frac{\overline{u}}{U_H}$ (a-c) between LDV and PIV measurements, at the three measurement locations on the roof (R_A, R_B, R_C) of the bare building with two side wall openings.

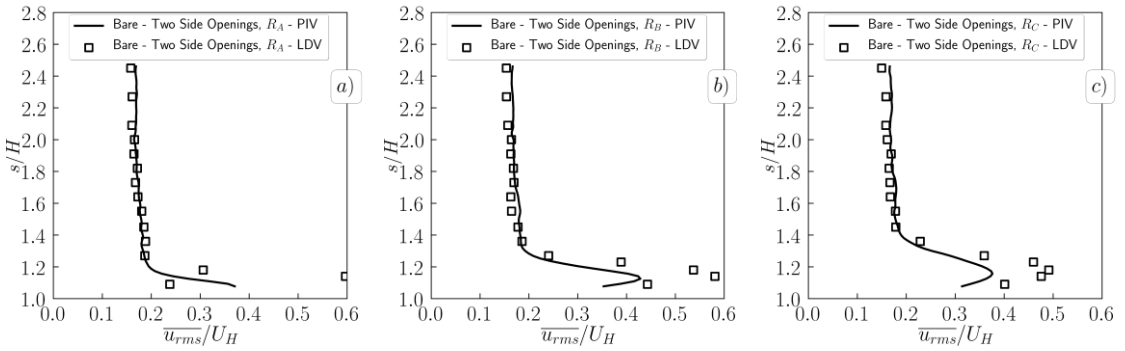

Figure 6. Comparison of the vertical profiles of the non-dimensional *rms* streamwise velocity component, $\frac{\overline{u_{rms}}}{U_H}$, between LDV and PIV measurements, at the three measurement locations on the roof (R_A, R_B, R_C) of the bare building with two side wall openings.

2.3.2 PIV flow field on the roof and in the wake

Figure 7a-h show the Stereo PIV planes which were measured asynchronously on the roof and in the wake, in the *x-y* symmetry plane, for the eight investigated cases : i) bare building without side wall openings, ii) bare building with two side wall openings, iii) façade greening, λ_{fs} = 9.31 m^{-1},T_{2L}, iv) façade greening, λ_{fs} = 1.98 m^{-1},T_{2L}, v) façade greening, λ_{fs} = 1.86 m^{-1},T_L, vi) rooftop greening, λ_{fs} = 9.31 m^{-1},T_{2L}, vii) rooftop greening, λ_{fs} = 1.98 m^{-1},T_{2L} and viii) rooftop greening, λ_{fs} = 1.86 m^{-1},T_L. Interest is now focused on the roof planes, giving an emphasis on the critical points of the flow, including the center of the recirculation bubble, F_t and the length of the reattachment region, X_{RR}/H. These results are from the NTUA wind tunnel where the boundary layer height, δ_{NTUA} is equal to 0.8 m, and δ/H = 7.3 represents a thick boundary layer. The corresponding parameter in the KIT wind tunnel (δ_{KIT} = 0.5 m) is δ/H = 4.5 (again, a thick boundary layer). The contours of Figure 7 represent the non-dimensional mean streamwise velocity, $\frac{\overline{u}}{U_H}$ along with the streamlines of the 3D velocity field. The flow structure above the roof changes significantly and shows different topologies depending on the presence or absence of the side wall openings, the position of the

Co-funded by the European Union

implanted vegetation (windward façade or rooftop greening) and the vegetation permeabilities and thicknesses. To facilitate comparison the streamwise, x/H and vertical, y/H coordinates of the center of the recirculation bubble, F_t and the total length of the reattachment region, X_{RR}/H are presented in Table 3 for all tested configurations. It seems that the distance between the roof level and the center of the recirculation bubble is not affected by the presence of the apertures or windward façade greening. The presence of rooftop greening inevitably determines the vertical distance as the inclusion of vegetation on the roof increases the total height. The streamwise position of the recirculation bubble's center also seems to remain unaffected by the presence of the openings but this is not the case when greening is present. The presence of vegetation on the windward face or the roof causes the recirculation bubble to move further downstream compared to the baseline scenario, i.e. the model building with two side wall openings. This is an indication of flow through or bypassing the greening layer. The lower the pressure loss coefficient of the vegetation layer, the more flow will pass through it. On the other hand, thick and/or dense layers with high pressure loss coefficient will favour flow bypass of the vegetation layer. From the tested cases of both greening positions (windward façade and rooftop) and the information in Table 3,Table 7 it is evident that the greening layers with the higher permeability (lower pressure loss coefficients) cause the recirculation bubble to move further downstream. For the same permeability, the thicker layers lead to a larger downstream displacement. This mobility of the recirculation bubble maybe attributed to the flow through or bypass of the vegetation layers : the thicker greening layers of the higher permeabilities allow a significant part of the flow to pass through, compared to the same thickness at lower permeability. For the low permeability cases, which are closer to real world vegetation, a thinner greening layer allows a stronger effect of the entrance effects, which induce a higher pressure loss, encourage flow bypass of the greening layer and moves the recirculation bubble upstream.

From Table 3, discernable differences in the length of the reattachment region can be observed in the model building cases with and without apertures ($\Delta X_{RRrel} \sim 12.5\%$). For the windward façade greening, the most pronounced value comes from the λ_{fs} = 1.98 m^{-1},T_{2L} corresponding to 60% higher value for the same permeability but thinner greening layer and 25% higher value for the thicker and higher pressure loss coefficient value (λ_{fs} = 9.31 m^{-1}, T_{2L}). For the rooftop greening, it is always the case of the thicker layer with the higher pressure loss coefficient value (λ_{fs} = 9.31 m^{-1}, T_{2L}) where the largest reattachment length appears. This value is also the highest between all of the eight tested cases, while the minimum is found in the thinner greening cases with higher permeability values (lower pressure loss coefficient). One parameter which is directly related to the mobility and the increase of the reattachment point position is the incoming turbulence intensity at cube height [8, 9]. In the present experiments, it is generally accepted that all the tested cases were performed under the same incoming turbulence intensity profile as the one presented in Figure 2b with a nominal turbulence intensity at cube height equal to $I_u \sim 19$ %. However, the fact that the windward façade was completely covered by the vegetation layer ($A_{coverage}$ = 100 %) and this was also the case with the rooftop greening means that the cube edges were in some way affected by the existence of the vegetation and that they locally changed the turbulence intensity in the flow direction. An indication of this behavior is probably the location of the roof reattachment point, X_{RR}.

Co-funded by the European Union

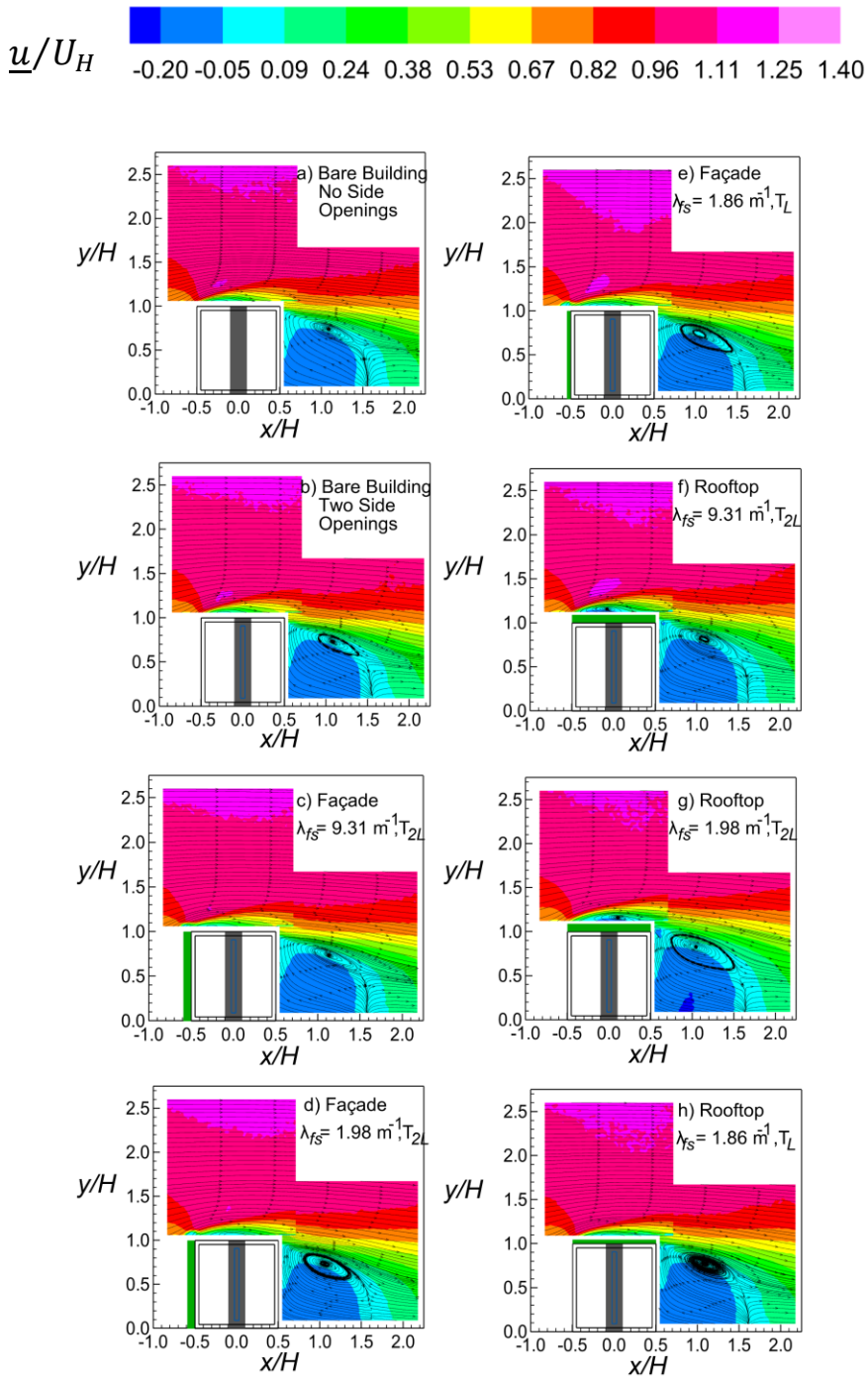

Figure 7. Non-dimensional mean streamwise velocity component ($\frac{\overline{u}}{U_H}$) and in-plane flow lines on the PIV planes along the model building centreline (roof and wake planes) for all tested cases.

Co-funded by the European Union

Table 3. Location of the center of the recirculation bubble and the length of the reattachment region on the roof, as identified in Figure 7.

$\delta_{NTUA}/H = 7.3$	Center of recirculation bubble, F_{R_i}			Length of roof reattachment, X_{RR}
Tested cases	x/H	y/H	z/H	X_{RR}/H
Bare (No Openings)	−0.36	1.06	0.0	0.29
Bare (Two Side Openings)	−0.36	1.06	0.0	0.25
Façade, $\lambda_{fs} = 9.31\ m^{-1}$, T_{2L}	−0.39	1.06	0.0	0.19
Façade, $\lambda_{fs} = 1.98\ m^{-1}$, T_{2L}	−0.16	1.06	0.0	0.24
Façade, $\lambda_{fs} = 1.86\ m^{-1}$, T_L	−0.20	1.06	0.0	0.10
Rooftop, $\lambda_{fs} = 9.31\ m^{-1}$, T_{2L}	−0.07	1.16	0.0	0.48
Rooftop, $\lambda_{fs} = 1.98\ m^{-1}$, T_{2L}	0.15	1.16	0.0	0.43
Rooftop, $\lambda_{fs} = 1.86\ m^{-1}$, T_L	−0.13	1.09	0.0	0.10

In addition, a comparison between the LDV and the PIV measurements at the three measurement locations on the roof (R_A,R_B,R_C) is presented in Figure 8 , similar to the approach in Figure 5, but now including the tested façade greening cases. It is extremely interesting that both measurement methods show the same behavior and detect even small changes when greening layer of different permeabilities are tested. The major differences between the reference and the greening cases are observed up to s/H = 1.3 which is the upper edge of the recirculation bubble for both LDV and PIV results.

Co-funded by the European Union

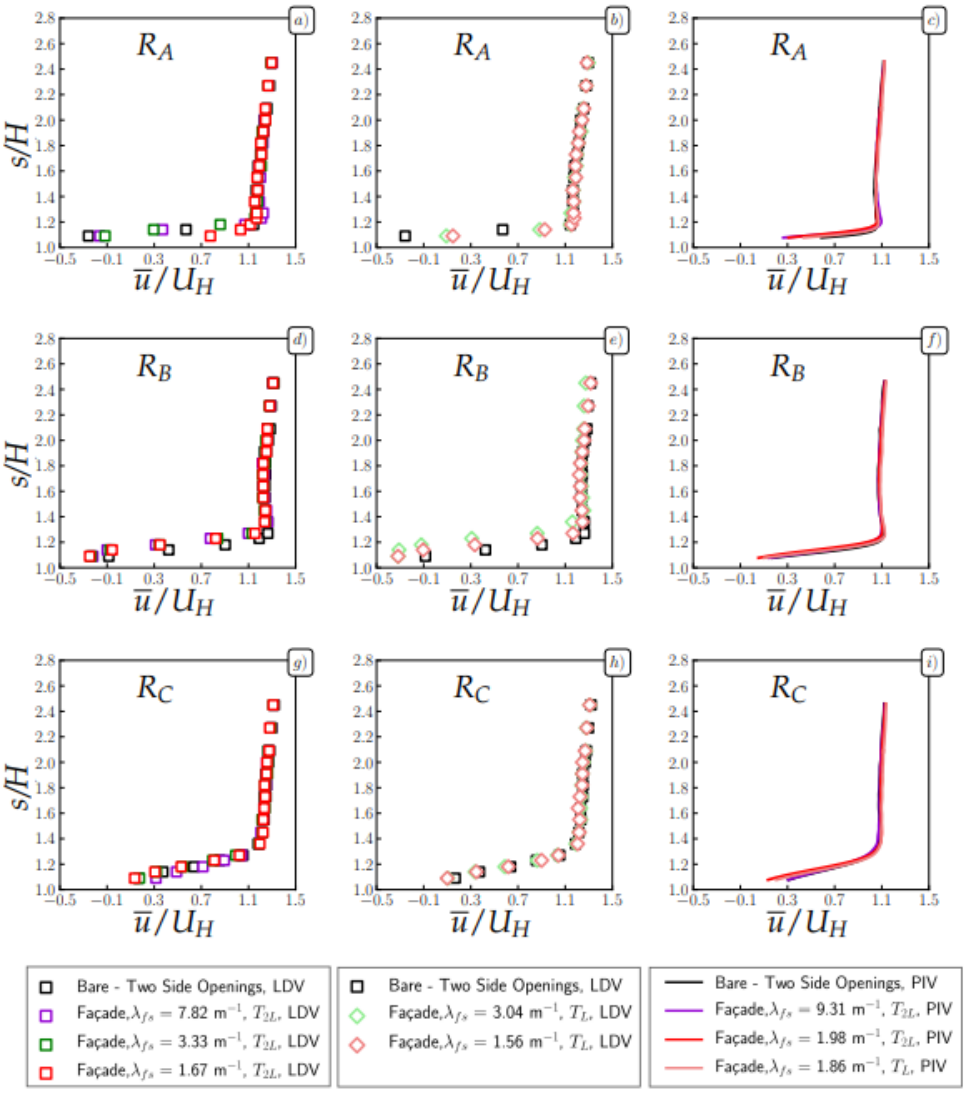

Figure 8. Comparison of the vertical profiles of the non-dimensional mean streamwise velocity, $\frac{\overline{u}}{U_H}$ between LDV - greening of Double thicknesses , LDV - greening of Thicknesses and PIV greening (all thicknesses) measurements, at the three measurement locations on the roof (R_A, R_B, R_C) for all tested cases.

2.4 Conclusions

A twin wind tunnel test has been performed for the flow past a building with or without greening on its windward façade or rooftop. Measurements were performed at two wind tunnels, ensuring matching upstream boundary layer profiles and building geometry. Measurement results provide insight into the effects of building outer surface greening on the flow and an opportunity to evaluate sources of discrepancy when measuring the same setup in different wind tunnels. The results indicate that although there may be a high level of sensitivity to the upstream flow profile when comparing absolute values of the flow characteristics, the same effects of surface greening are captured in the two measurement sets.

Co-funded by the European Union

3 Twin Test 2: Wake Interactions of a Cluster of Turbines and Wake Steering Techniques

3.1 Introduction

Twin Test 2 (TWT2) is an experimental campaign conducted at the wind tunnel facilities of the Technical University of Munich (TUM), Germany, and the National Technical University of Athens (NTUA), Greece. The experiments focus on the aerodynamic interaction between two wind turbine models, with a particular emphasis on the effectiveness of two wake control strategies: Individual Pitch Control (IPC) and wake steering through static yaw misalignment.

To ensure high-quality measurements and enhance the interaction and knowledge exchange, state-of-the-art instrumentation provided by Delft University of Technology (TU Delft) was employed during the tests at NTUA. The campaign aims to support knowledge exchange between the project partners and to generate new knowledge into wake control mechanisms and turbine interactions under controlled wind tunnel conditions.

This deliverable presents and compares the experimental results obtained at the two facilities, assessing the consistency between datasets and identifying key findings related to wake behavior and control performance. For further information, please refer to the TWT2 TWEET-IE book of reference [10] or the zenodo database [11].

3.2 Experiment description

The experiments were conducted in the closed-loop, low-speed boundary layer wind tunnel at TUM and in the large section of the closed-circuit wind tunnel at NTUA. The set up consists of two identically scaled wind turbine models, placed in line with a longitudinal distance of 5D, where D denotes the rotor's diameter. Figure 9 represents the experimental setup at TUM, similar to that of NTUA, showing the static pressure taps located at the centre (y=0) of the wind tunnel ceiling, the location of the pitot tube as well as the wind turbine models [12].

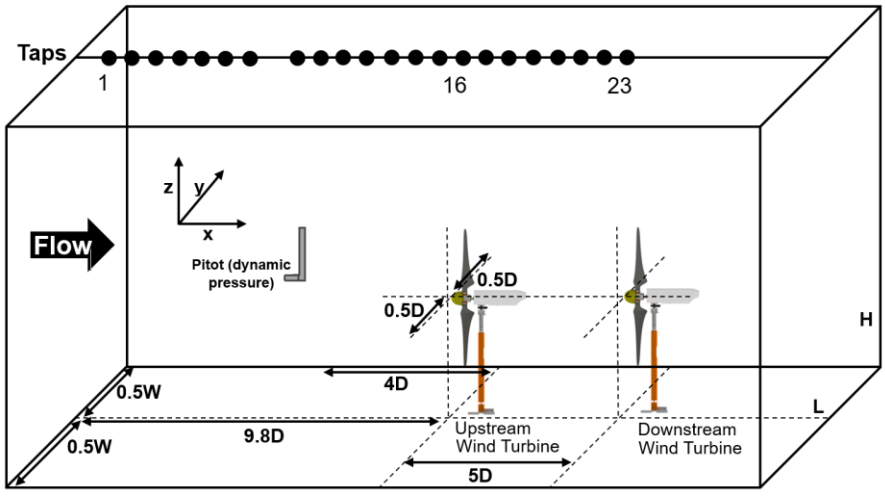

Figure 9. Sketch of the wind tunnel test section at TUM with the positioning of the pressure taps in the centre of the wind tunnel ceiling, the location of the pitot tube and the locations of the upstream and downstream wind turbine models.

Co-funded by the European Union

The upstream turbine was initially tested in its baseline configuration before being subjected to dynamic helix motion, with amplitude ranges of 3° and helix frequency of $f_{helix} = \frac{f_\beta}{f_r} \in [0.7,1.3]$, where $f_\beta = f_r \pm f_e$ represents individual sinusoidal blade excitation frequency, $f_r = 1P$ is the rotational frequency and f_e is the additional excitation frequency, which is either added to or subtracted from the rotational frequency, leading to the CCW or CW wake meandering, respectively [13,12].

The turbine models used were the G1 turbines [14], developed by TUM, designed for precise performance characterization and equipped with advanced sensors for measuring torque, thrust, and other performance metrics. G1 features a rotor diameter of $D = 1.1$ m, a hub height of $z_{hub} = 0.82$ m, a rated rotor speed, $\omega = 850$ rpm (CW rotation) and a blade pitch $\beta \approx 0.4°$.

For all cases, the turbine power coefficient, $\mathbf{C_P}$, was calculated using equation 2.1

$$C_P = \frac{P}{0.5\rho U_{pitot}^3 \pi (0.5D)^2} = \frac{\omega T}{0.5\rho U_{pitot}^3 \pi (0.5D)^2} \tag{2.1}$$

where P is the power, ω is the rotor speed, T is the torque measured by the shaft strain gauges and U_{pitot} is the uncorrected wind tunnel velocity. The thrust coefficient, C_T, was calculated using equation 2.2 and finally, the Tip Speed Ratio (TSR) was calculated using equation 2.3:

$$C_T = \frac{Thrust}{0.5\rho U_{pitot}^2 \pi (0.5D)^2} \tag{2.2}$$

$$TSR = \frac{\omega D}{2U_{pitot}} \tag{2.3}$$

3.3 Results

Since the goal of the twin tests is to accurately replicate identical experiments in different environments, it is essential to evaluate and compare the performance of the wind turbines across the two wind tunnels. As a first step, the power coefficient C_P was assessed for the baseline configuration, where no active wake control strategy was applied.

The two tunnels differ significantly in cross-sectional area, resulting in notable blockage effects, approximately 19.6% at TUM and 10.9% at NTUA. To enable a meaningful comparison between the measurements, a blockage correction was applied. As shown in Figure 10a, there is a substantial discrepancy in C_P between the two turbines before correction, particularly for the upstream turbine. However, after applying the blockage correction (Figure 10b), the datasets align closely for both turbines. This indicates that the airflow is significantly – and differently – accelerated around the rotor in each tunnel due to the frontal area of the models, highlighting the importance of accounting for blockage effects in such comparisons.

Co-funded by the European Union

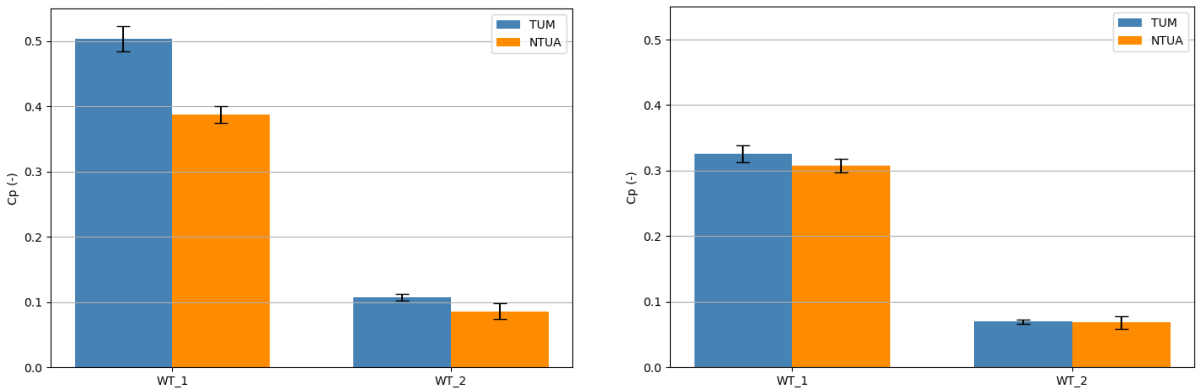

a) Uncorrected results b): Blockage corrected results

Figure 10: Power coefficient comparison between the two wind tunnels for the baseline configuration.

As a next step, the helix active wake control strategy was implemented on the upstream wind turbine. The uncorrected power measurements (Figure 11) show that both tunnels exhibit a similar trend for each turbine; however, there remains a notable difference in the absolute values. After applying the blockage correction (Figure 12), the power output of the upstream turbine aligns almost perfectly between the two facilities, falling within the measurement uncertainty. For the downstream turbine, the corrected results also show improved agreement, particularly in the frequency range $f_{helix} = [0.9,1.1]$, where the curves closely match. Outside this range, however, discrepancies still persist across the two datasets.

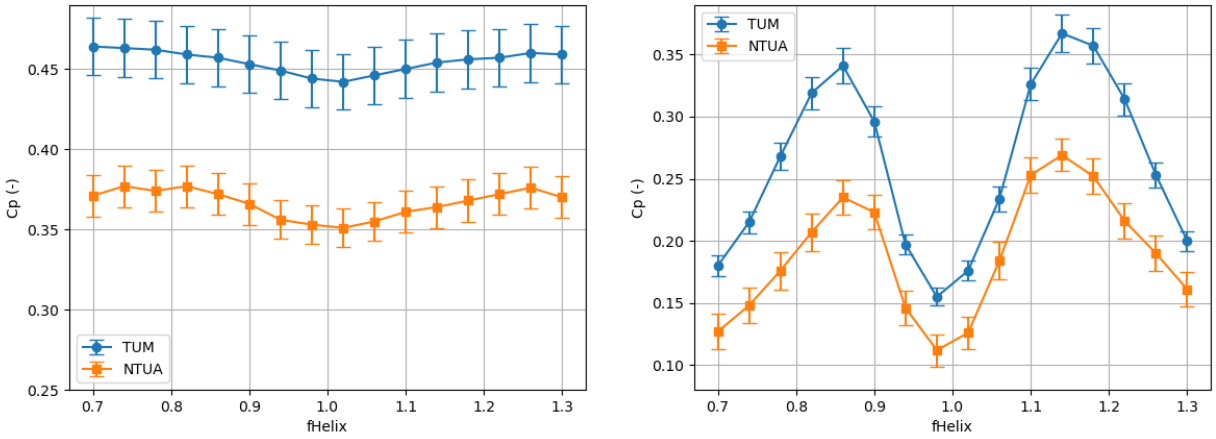

a): Upstream Wind Turbine b): Downstream Wind Turbine

Figure 11: Power coefficient comparison between the two wind tunnels for the helix configuration – Uncorrected results.

Finally, Figure 13 presents the normalized total power output of the two-turbine array relative to their respective baseline reference values. This comparison enables the assessment of the helix wake control strategy's effectiveness against the baseline scenario. The results from both wind tunnels show a strong correlation, consistently indicating improved performance across most helix frequencies. Notably, two distinct performance peaks are observed at $f_{helix} = 0.86$ and $f_{helix} = 1.14$, with the latter representing the global optimum in terms of power enhancement.

Co-funded by the European Union

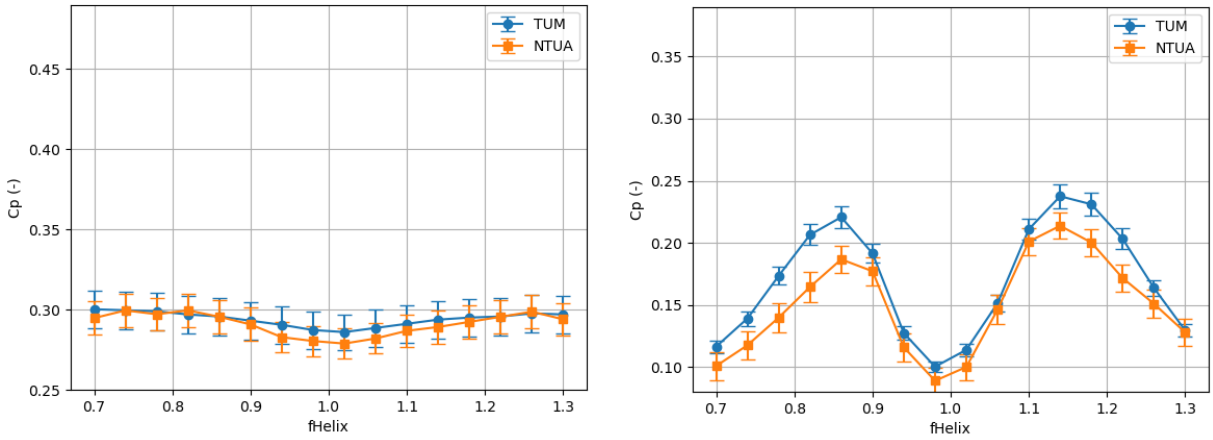

a) Upstream Wind Turbine b) Downstream Wind Turbine

Figure 12: Power coefficient comparison between the two wind tunnels for the helix configuration – Blockage corrected results.

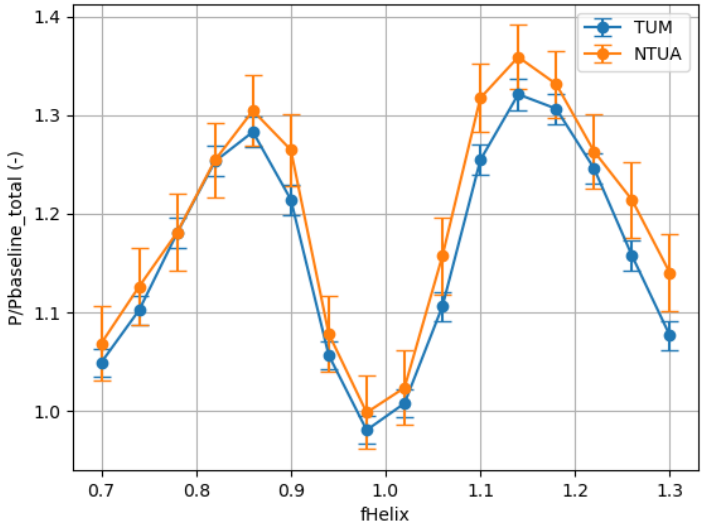

Figure 13. Normalized power versus helix frequency for the total of wind turbines.

3.4 Additional Wind Tunnel Tests

At the beginning of the project it was agreed that the topic of wake control was of great interest for all partners working in wind energy and as such it was decided to extend the twin test comparisons to two additional wind tunnels at no expense to the project. The additional tests were performed in July 2025 at the large wind tunnel facility in Politecnico di Milano and will be performed in September 2025 in the Open Jet facility in TU Delft.

The additional tests offer the following advantages. First, the wake control techniques will be tested in a facility with very small blockage (approx. 1% in POLIMI). This will provide greater confidence for the measurements performed both at NTUA and at TU Munich. Second, the tests at TU Delft will provide

Co-funded by the European Union

greater insight and knowledge with regards to the early development of the wake (1D-2D) as larger area PTV measurements are planned.

3.5 Conclusions

Wind turbine performance wind tunnel tests were performed for two aligned wind turbine models in two different wind tunnel facilities. The main differences between the two facilities are the blockage ratio and the inflow profiles. The results match very well between the two facilities when corrected for blockage using established methods suggested in the literature. Further experiments planned at two more facilities are expected to provide greater confidence in the results as well as new knowledge.

Co-funded by the European Union

4 Twin Test 3: Micro devices for Enhanced Performance of Airfoil Sections

4.1 Background & Introduction

In this TWT campaign, Twin Tests were conducted assessing the effect of micro devices for enhanced performance of flatback (FB) airfoil sections. FB airfoils, i.e. thick airfoils with a blunt trailing edge (TE) are used near the root region of modern wind turbine blades, as they provide several benefits compared to their thin TE counterparts [15]. The utter goal is to elucidate the effect of freestream turbulence intensity, Reynolds number and blockage ratio on airfoil performance, 3D flow separation and wake behaviour. Additionally, the effect of flow control devices regarding flow separation control and drag reduction were assessed. However, in this report, we focus on establishing and comparing the baseline case between facilities.

4.2 TWT Setups

4.2.1 The model

The model is a three-dimensional rectangular wing of the FB4286-0802 airfoil, a FB airfoil with a maximum thickness that is 42.86% of the chord length and a trailing edge height of 8.02% of the chord length. The profile of the FB4286-0802 is shown in Figure 14. The physical model is made from polyurethane and has a chord length of 0.5m and a span of 1m, i.e. the aspect ratio of the wing model is 2. Additionally, the model is fitted with 63 pressure taps.

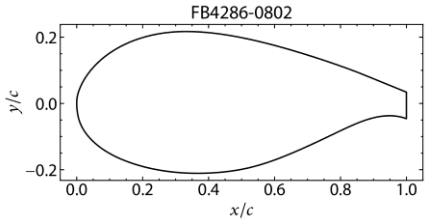

Figure 14. The FB4286-0802 profile.

4.2.2 NTUA Setup

Tests are carried out at the small test section of the closed-loop Wind Tunnel of the National Technical University of Athens (NTUA). The test section is 3.75m long and has an octagonal cross-section of main dimensions 1.8m × 1.4m (width × height). The maximum wind speed is 45m/s, with a turbulence intensity (TI) lower than 0.2% and the blockage ratio is 11.9%. The model is fitted with endplates and wooden extensions spanning the entire test section vertically, as shown in Figure 15a.

The NTUA tests consist of surface pressure measurements, hot-wire measurements, flow visualization with tufts and Stereo Particle Image Velocimetry (SPIV) measurements. The pressure measurements allow for determining the basic performance characteristics of the airfoil, and the hot wire measurements provide information about the primal shedding frequency. Additionally, the tufts help to understand the three-dimensional effects due to flow separation and the SPIV measurements provide a basic

Co-funded by the European Union

understanding of the wake structures. Both fixed and free transition cases are tested at a single Reynolds number of Re = 1.25M.

4.2.3 POLIMI Setup

The tests for POLIMI will be conducted in the Low Turbulence Test Section of the Galleria del Vento del Politecnico di Milano (GVPM). The facility is a closed-loop wind tunnel and the utilized test section measures 4m in length with a cross-section of 4m × 3.84m. The maximum wind velocity is 55m/s, with a free-stream TI level below 0.1%, while the blockage, with this model, is about 1.88%. The model is fitted with endplates at the top and bottom, leaving a gap of 5mm between the model and each endplate, as shown in Figure 15b.

The POLIMI tests consist of surface pressure measurements, force balance and hot-wire measurements. The pressure measurements allow for determining the basic performance characteristics of the airfoil as well as comparing facilities. Next, the force balance measurements provide insights on the effect of the 3D separation to the airfoil loads and the hot-wire measurements allow for determining the spanwise wake correlations. Both fixed and free transition cases are tested at a single Reynolds number of Re = 1.25M.

(a) (b)

Figure 15. The two wind tunnel set-ups. (a) Front view of the NTUA setup. The model and the black endplates can be seen. The extensions placed at the top and bottom make the setup wall to wall. (b) The POLIMI setup. The model and the black endplates can be seen. The balance fairing is also visible in the bottom of the model.

A more detailed description of the setups can be found in Table 4 below. For the fixed transition cases, zig zag tape with a height of h_{zz} = 0.125mm was placed at 5% and 10% chord lengths of the suction and pressure sides, respectively. Additionally, different flow control devices were assessed during the TWT. Although not discussed in depth in this report, a summary of the investigated setups can be seen in Table 5. More detailed descriptions of the setups can be found in the corresponding Book of References.

Co-funded by the European Union

Table 4. Summary of the TWT

	NTUA	POLIMI
Blockage	12%	2%
Turbulence Intensity	<0.2%	<0.1%
Reynolds number (x1M)	1.25	1.25
Surface Pressure	✓(32/63 taps)	✓(63/63 taps)
Balance	×	✓
Hot-wire	✓(single)	✓(triple)
Tufts	✓	✓
StereoPIV	✓	×

Table 5. Summary of the setups investigated.

	NTUA	POLIMI	Notes
Baseline	12%	2%	
Baseline – Fixed Transition	<0.2%	<0.1%	h_{zz} = 0.125mm
Vortex Generators near max. thickness	1.25	1.25	Separation Control
Vortex Generators near trailing edge	✓(32/63 taps)	✓(63/63 taps)	Drag Reduction
Tabs near trailing edge	×	✓	Drag Reduction
Gurney flaps	✓(single)	✓(triple)	Lift increase

4.3 Results & Discussion

In this section we highlight the baseline results of the TWT, focusing on the airfoil polars. More details regarding the post processing of the experiment data and wake behaviour can be found in the corresponding Book of References.

4.3.1 Free Transition

Firstly, we present the results for the free transition case. The variation of the Lift force coefficient (C_L) and the Drag force coefficient (C_D) with the angle of attack (AoA) for the two facilities can be seen in Figure 16. Regarding C_L, an agreement is shown at low AoAs but the results obtained at NTUA indicate that the airfoil stalls much earlier (at around 6°) compared to the results from POLIMI (at 18°). Additionally, comparing the C_L obtained from pressure measurements compared to the one obtained from balance measurements at the POLIMI campaign, a difference in the standard deviation can be seen at high AoAs. This is a consequence of the present of three-dimensional separation structures near the bottom and top tips of the model, while the flow remains attached at the mid span area. This was verified using tuft flow visualization. Tufts, also revealed the presence of a pair of stall cells at the mid span location for the NTUA campaign, i.e. the three-dimensional separation structures appear differently in the two facilities. Regarding C_D, the drag in the POLIMI facility measured with balances is higher than the one estimated using the pressure measurements, as expected. Additionally, C_D at NTUA is lower than the one measured at POLIMI. This difference stems from the different pressure distributions at NTUA and POLIMI. For instance, in the right panel of Figure 16 the pressure coefficient (C_P) distribution can be seen for the two facilities at approximately 2°. The distributions are similar for the two facilities, with two major

Co-funded by the European Union

differences, near maximum thickness of the airfoil (10% to 30% of the chord), the extent of the pressure difference between the suction and pressure sides of the airfoil is higher at NTUA, leading to higher lift. While the flow re-attaches at around 90% of the chord at the pressure side for the POLIMI tests, leading to higher drag.

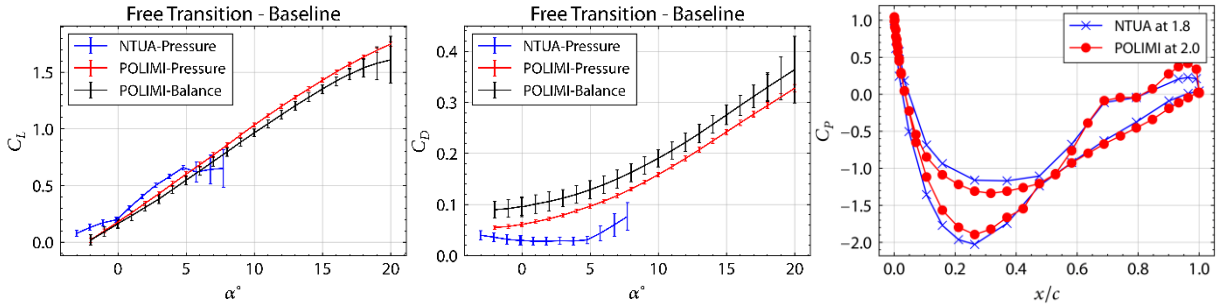

Figure 16. Performance for the free transition case. Left: C_L vs AoA , middle: C_D vs AoA, and right: C_P at 2°.

4.3.2 Fixed Transition

Next, we present the results for the fixed transition case. The variation of the Lift force coefficient (C_L) and the Drag force coefficient (C_D) with the angle of attack (AoA) for the two facilities can be seen in Figure 17. The flow separates much earlier compared to the free transition case. The results from the two facilities show three different regions regarding C_L: a region where lift increase - the flow is separated only at the pressure side, a region with negative lift slope (a trend observed in very thick airfoils [15]) where the flow is separated at both sides of the model and a region where lift is increasing with AoA but the flow is separated and the separation point keeps moving upstream. It is also noteworthy that there seems to be an offset of 4° between the development of these regions between the two facilities. It is also worth mentioning that a bifurcating behavior can be observed in both facilities just after the global C_L minimum. For example, the timeseries of pressure coefficient for a pressure tap located (x ,y) = (48%, 20%) of the chord at 10° for the POLIMI campaign can be seen in the right panel of Figure 17.

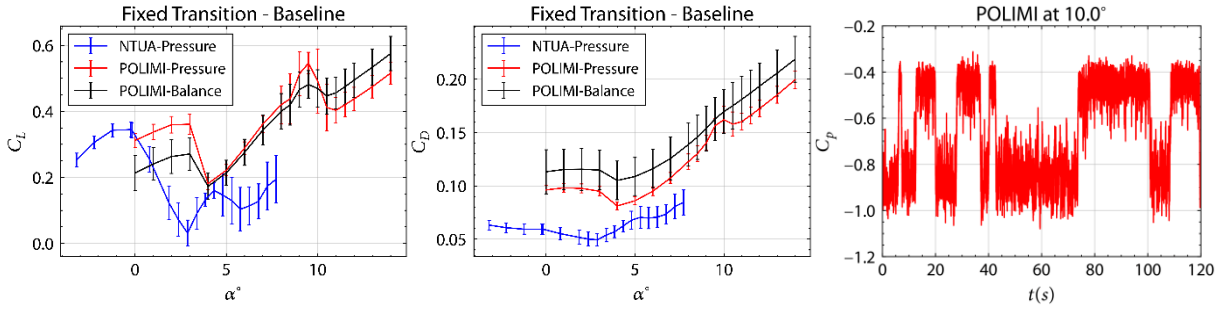

Figure 17. Performance for the fixed transition case. Left: C_L vs AoA , middle: C_D vs AoA, and right: C_P timeseries at 10° for the POLIMI campaign for a pressure tap located in (x/c, y/c)=0.48, 0.2).

Co-funded by the European Union

4.4 Conclusions

A flatback airfoil section (FB4286-0802) was tested under matched Reynolds number and transition conditions at two distinct facilities: NTUA and POLIMI. The primary objective was to assess consistency across facilities and to understand how different wind tunnel environments, specifically turbulence intensity and blockage ratio, influence aerodynamic performance and three-dimensional flow behavior.

The results highlight that while the general trends of lift and drag behavior are consistent between the two facilities, there are significant differences in lift and drag values, mainly related to aspects such as stall onset and separation behavior. In free transition conditions, POLIMI's setup exhibited delayed stall and higher drag, whereas NTUA demonstrated earlier stall and stronger suction peaks—likely influenced by its higher blockage ratio and wall-to-wall setup. These factors resulted in differing three-dimensional flow structures, such as stall cells, as observed in tuft flow visualization tests. Under fixed transition conditions, both setups revealed more pronounced flow separation and complex lift behavior, including regions of negative lift slope and bifurcation in pressure signals.

Overall, the campaign highlights the importance of cross-facility comparisons in experimental aerodynamics, especially for airfoil configurations like very thick flatback profiles that are highly sensitive to 3D separated flow. The established baselines provide a solid foundation for future studies involving flow control devices and offer valuable insights for the design and validation of wind turbine blades employing thick root airfoils.

Co-funded by the European Union

5 Twin Test 4: Scale Effects in Urban Flows

5.1 Introduction

The current twin test (TWT4) consists of an investigation of the scale effects on flow in the urban environment. More specifically, this urban environment is a series of five consecutive identical street canyons perpendicular to the approaching flow, simulating the urban fabric. Measurements have been carried out in the closed-type wind tunnel (WT) facility[1] of the National Technical University of Athens (NTUA) as well as in the open jet facility[2] (OJF) of TU Delft. The measurement equipment was mainly provided by TU Delft.

The examined canyon was the fourth one with respect to the direction of the approaching flow. The effect of vegetation (hedges at the pedestrian level or roof greening) on the flow is also examined throughout this study. In the WT of NTUA, all the former cases were investigated for two different values of ambient turbulence intensity corresponding to two distinct experimental configurations (i.e. with and without a passive grid). The study at NTUA was performed with a 3D-3C Robotic Particle Tracking Velocimetry (3D-PTV) System and at TU Delft with a 3D-3C Volumetric PTV system. Both systems can be categorised as volumetric methods. Additionally, surface pressure measurements were conducted in both wind tunnels whereas hot-film anemometry was employed in NTUA's WT to supplement the PTV-extracted dataset. The height-to-width (W/H) and the length-to-width (L/W) aspect ratios of the street canyons are 1 and 8, respectively, for both experiments. For more details the reader is referred to [16] and [17].

5.2 Experiment description

An urban street canyon configuration consisting of 5 subsequent street canyons with aspect ratios W/H =1 and L/H = 8 was tested in both facilities i.e. at NTUA and TU Delft. Scale effects were investigated mainly in the region that was in the vicinity of the fourth canyon (examined canyon). The coordinate system, the basic dimensions of the model as well as its orientation with respect to the approaching flow are shown in Figure 18a. The red line, shown in Figure 18a, corresponds to the location of surface pressure measurements conducted in the framework of the same experimental campaign. These measurements were performed in both facilities. The model was mounted onto a splitter plate to eliminate boundary-layer effects originating from the floor of the wind tunnel. A top view of the model is given in Figure 18b where the splitter plate as well as some additional structural details (related to the NTUA setup) are also shown.

For the simulation of vegetation, porous material (foam) with PPI20 (i.e. 20 pores per inch) was used for both the hedges and the roof greening. The vegetation modelling procedure was the same as in the TWT1, presented in section 2. More details regarding the modelling of vegetation are given in [18]. A Schematic illustration of the position of vegetation with respect to the examined canyon along with the necessary dimensions is given in Figure 18c.

[1] http://wt.fluid.mech.ntua.gr/
[2] https://www.tudelft.nl/lr/organisatie/afdelingen/flow-physics-and-technology/facilities/low-speed-wind-tunnels/open-jet-facility

Co-funded by the European Union

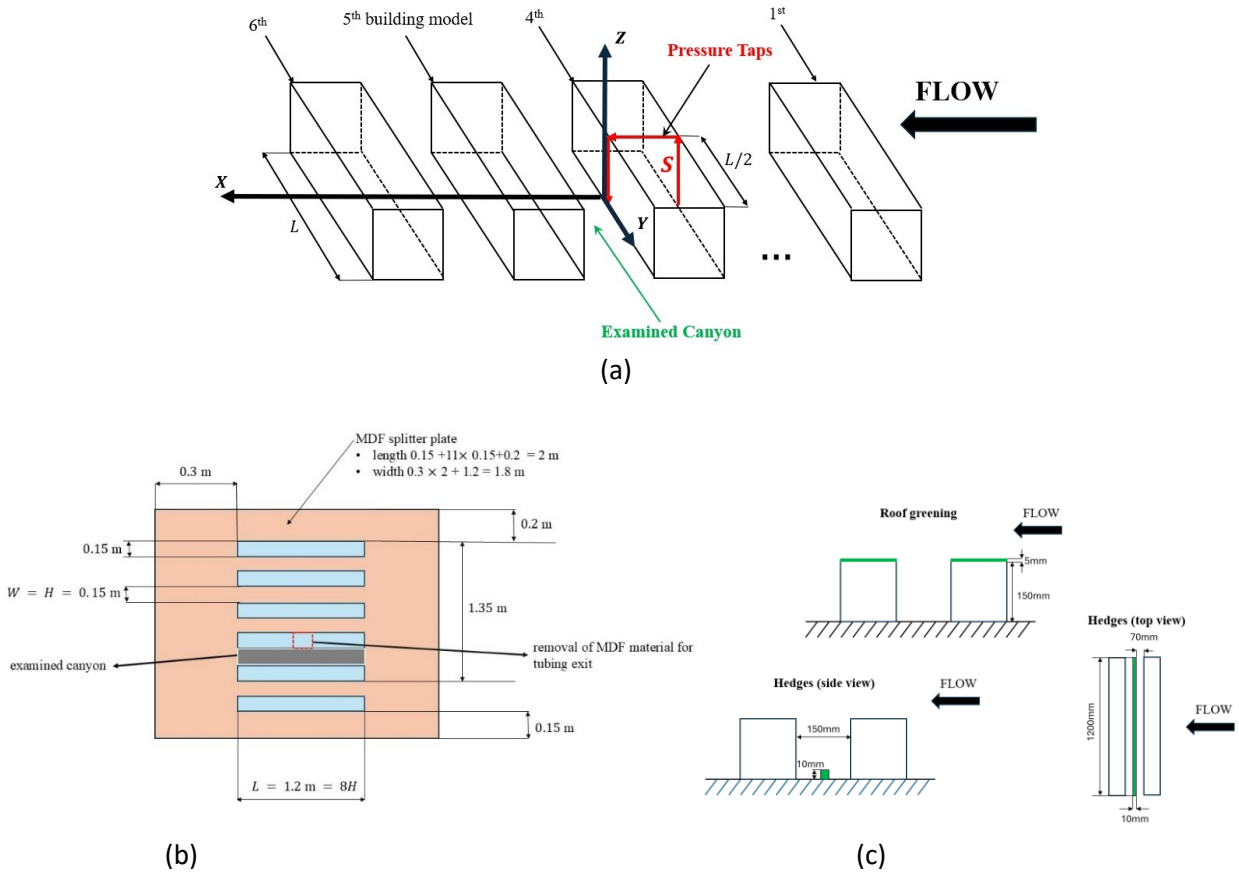

Figure 18. (a) schematic illustration of: (a) the model and the coordinate system (3D view), (b) the model along with some structural details and (c) the position of vegetation with respect to the examined canyon along with the necessary dimensions.

5.2.1 NTUA setup

The present test was performed in the 3.5 m x 2.5 m x 12.1 m test section of the wind tunnel facility of the National Technical University of Athens. An increased value of ambient turbulence intensity was achieved by applying a passive turbulence grid to the inlet of the test section. This enabled the undertaking of measurements in conditions of low (~1%) and high (5-6%) ambient turbulence intensity (TI).

Time-averaged velocities (streamwise, vertical and lateral) as well as their standard deviations have been extracted by means of Robotic 3D-3C PTV. The Robotic 3D-3C PTV system consists of a Coaxial Volumetric Velocimetry (CVV) probe mounted on a Universal Robots UR5 robotic arm with six degrees of freedom (3 rotations and 3 translations). For more details regarding the CVV probe, the readers are referred to [19] and [20].

Two LaVision LED Flashlight 300s were utilised to obtain sufficient pulsed volumetric illumination. Each module consists of an array of 72 high-power LEDs in an area of 300x100mm^2. Neutrally buoyant helium-filled soap bubbles [21] of 300 μm median diameter [22] were used as tracer particles for PTV.

Co-funded by the European Union

The PTV dataset is complemented by pressure measurements as well as Constant Temperature Anemometry measurements. The latter were conducted to: (a) characterise the developed boundary layer on the roofs of selected building models and (b) to quantify the approaching flow in front of the whole model.

5.2.2 TU Delft setup

The examined model was tested in the open jet facility of TU Delft. The size of the OJF outlet is 2.85 m x 2.85 m. Three high-speed Photron Fastcam SA1.1 cameras were used for the experiment. Time-averaged velocities (streamwise, vertical and lateral) as well as their standard deviations have been extracted as in the case of the NTUA experiment.

The same sources of illumination and seeding material as those in the NTUA test section were employed. PTV results were complemented by surface pressure measurements.

5.3 Test Matrix

The test matrices corresponding to the NTUA and TU Delft experiments are given in Table 6 and Table 7, respectively. The Reynolds number is defined as: $Re = U_{ref}H/\nu$, where U_{ref} is the free-stream velocity, H is the height of the building models, and ν is the kinematic viscosity of the air during the experiment.

Table 6. Test matrix containing the individual experiments conducted in the wind tunnel facility of NTUA.

Configuration	Re	Volume	TU Delft data
Bare canyon (low turb[3])	22,000	half of the canyon[4]	**no**
Bare canyon (low turb)	28,000	half of the canyon	**yes**
Bare canyon (low turb)	37,000	half of the canyon	**yes**
Bare canyon (low turb)	47,000	half of the canyon	**yes**
Bare canyon (low turb)	56,000	half of the canyon	**yes**
Hedge (low turb)	56,000	half of the canyon	**yes**
Roof greening (low turb)	56,000	half of the canyon	**yes**
Bare canyon (high turb[5])	23,000	half of the canyon	**no**
Bare canyon (high turb)	28,000	half of the canyon	**no**
Bare canyon (high turb)	37,000	half of the canyon	**no**
Bare canyon (high turb)	47,000	half of the canyon	**no**
Bare canyon (high turb)	57,000	half of the canyon	**no**
Hedge (high turb)	57,000	half of the canyon	**no**
Roof greening (high turb)	57,000	half of the canyon	**No**

[3] *Low Turb*: no passive grid is used for the increase of ambient turbulent intensity (TI). Therefore TI~1%.
[4] The volume was somewhat larger than half of the canyon in the Y direction. It also extended on the roofs of the buildings forming the examined canyon.
[5] *High Turb*: a passive grid is applied to the inlet of the test section to increase the ambient turbulence intensity (TI). Therefore TI~5-6%.

Co-funded by the European Union

Table 7. Test matrix containing the individual experiments conducted in the open jet facility of TU Delft.

Configuration	Re	Volume	NTUA data
Bare canyon	30,000	half of the canyon[6]	**yes**
Bare canyon	40,000	half of the canyon	**yes**
Bare canyon	50,000	half of the canyon	**yes**
Bare canyon	60,000	half of the canyon	**yes**
Bare canyon	80,000	half of the canyon	**no**
Bare canyon	100,000	half of the canyon	**no**
Hedge	40,000	around centre-plane	**no**
Hedge	60,000	half of the canyon	**yes**
Hedge	80,000	around centre-plane	**no**
Roof greening	40,000	around centre-plane	**no**
Roof greening	60,000	half of the canyon	**yes**
Roof greening	80,000	around centre-plane	**no**

5.4 Results

The three main goals of the presented experimental campaign are the following: (i) examination of scale effects in an urban street canyon configuration, (ii) investigation of the influence of vegetation in an urban street canyon configuration and (iii) comparison between the measurements from the two facilities. A brief presentation of the results pertaining to each of the above-mentioned scientific inquiries is given in this section. The focus here is mainly on the PTV results.

5.4.1 Scale Effects

PTV results extracted at NTUA are shown here and for TI~1%. Similar results (not shown here) are available also for TI~5-6% as well as the experiment conducted in TU Delft. In particular, Figure 19 shows contours of the normalised mean streamwise velocity component and velocity vectors for $Re = 22000$ and $Re = 56000$. The results pertain to the centre-plane ($Y/H = 0$, see Figure 18a) of the examined canyon.

Overall, no significant differences are obvious between the results of $Re = 22000$ and $Re = 56000$, except: (i) some small differences in the lower left corner where the secondary vortex is observed, (ii) for the higher Re number, there is a slightly stronger upward velocity component near the upper corner of the leeward wall of the canyon and (iii) the region of the most negative streamwise velocity (dark blue contour level) is smaller at $Re = 22000$. Note that scale effects have also been examined towards the lateral end of the canyon [16]. Conclusively, it has been observed that the general flow structure was Re-independent for both turbulence intensity scenarios at NTUA as well as at the examined cases at TU Delft.

[6] The volume was somewhat larger than half of the canyon in the Y direction. It also extended above the roofs of the buildings forming the examined canyon.

Co-funded by the European Union

However, local scale effects like the ones mentioned above were always present, indicating that higher Reynolds numbers may be required to ensure universal Re-independence in the whole examined volume.

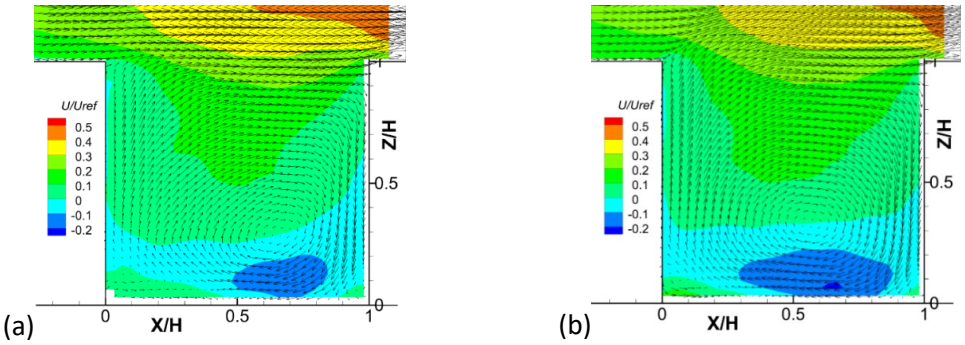

Figure 19. Velocity vectors (tangent) and contours of the normalised mean streamwise velocity component U/U_{ref} for: (a) $Re = 22000$ and (b) $Re = 56000$, in the centre-plane. The flow is from left to right, with $U_{ref} = U_{\infty}$.

5.4.2 Vegetation Effects

The influence of two types of vegetation, i.e. roof greening and hedges, was examined in the current twin test in both facilities. Here, results pertaining only to the low ambient turbulence intensity (TI~1.5%) are shown. More specifically, contours of the normalised mean streamwise velocity component along with velocity vectors are given for the centre-plane ($Y/H = 0$, see Figure 18a) of the examined canyon and for the: (a) bare canyon configuration, (b) configuration with roof greening and (c) configuration with hedge row at $Re = 56000$, in Figure 20.

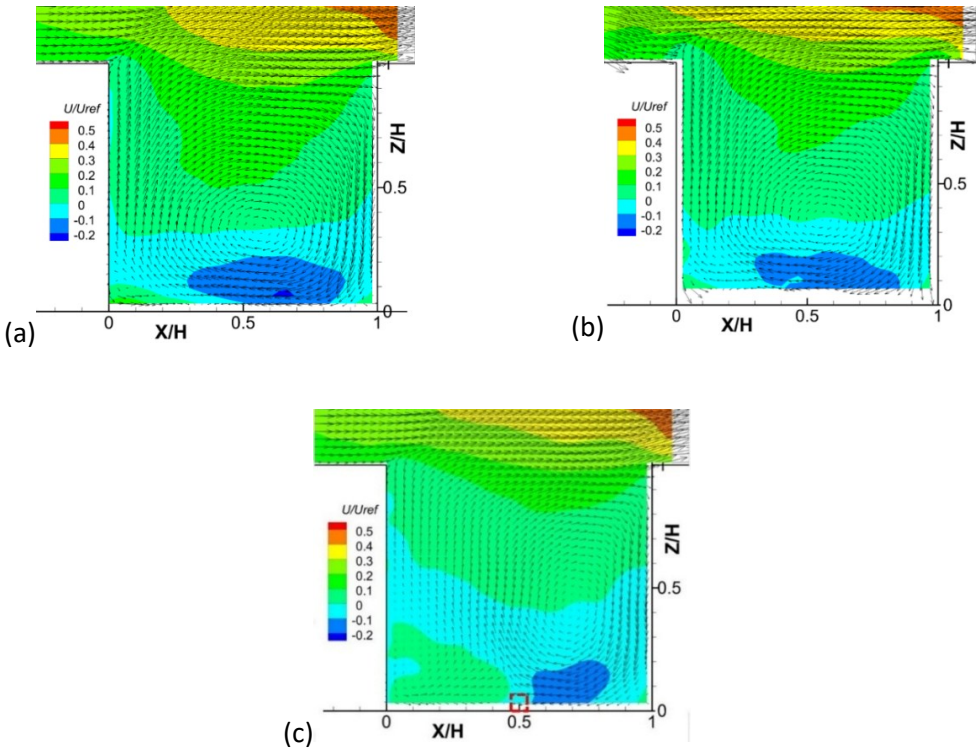

Figure 20. Velocity vectors (tangent) and contours of the normalised mean streamwise velocity component U/U_{ref} in the centre-plane of the canyon, for the: (a) bare canyon case, (b) configuration with roof greening and (c) configuration with the

Co-funded by the European Union

hedge row where the latter is indicated by the red dashed box. The flow is from left to right and the Reynolds number is equal to 56000 for all cases, with $U_{ref} = U_{\infty}$.

It is observed that the influence of roof greening on the flow inside the canyon is almost negligible. This is not the case though for the configuration with the hedge row. More specifically, the flow structure is clearly different from that of the bare canyon case since: (i) the position and the shape of the main canyon vortex changes under the influence of the hedge row and (ii) the secondary vortex in the lower left corner is clearly larger for the hedge row configuration. Similar behaviour is observed also for TI~5-6%. For the TU Delft experiment, the processing of the respective cases is ongoing.

5.4.3 Comparison between NTUA and TU Delft results

The flow structure between the NTUA and TU Delft experiments is drastically different, i.e. in the former case there is a vortex located at the centre-plane while in the latter case there is not one. The comparison is shown in Figure 21 for $Re \approx 60000$ (in NTUA the exact value was 56000), for the centre-plane ($Y/H = 0$, see Figure 18a) of the examined canyon by means of contours of the normalised mean streamwise velocity component along with velocity vectors. Another striking difference, discernible in Figure 21, is related to the existence of a wide recirculation region near the roof of the upstream building at TU Delft. The regions pertaining to the forenamed differences are encircled in black and red, respectively. In general, the difference in the structure of the flow can be attributed to the different types of facilities i.e. open jet (TU Delft) and enclosed (NTUA) wind tunnel test section. More details are given in the next section.

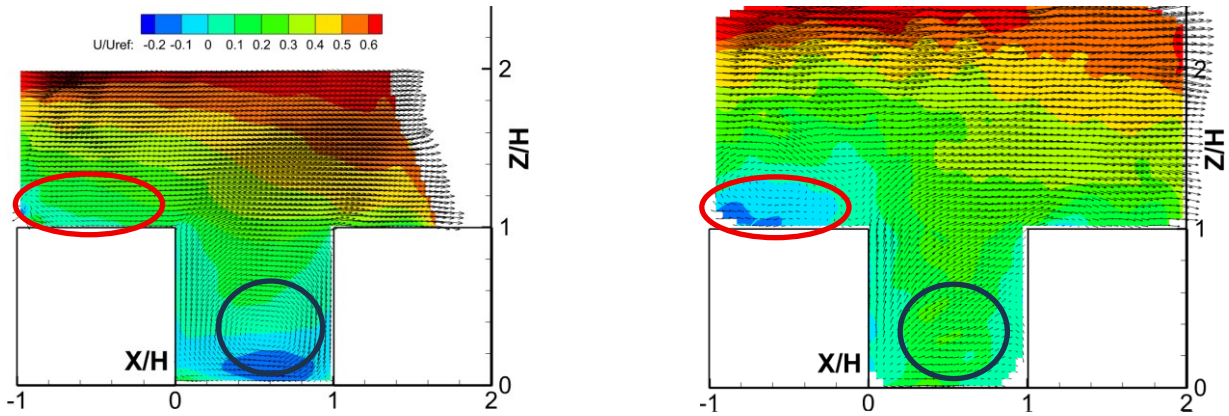

Figure 21. Velocity vectors (tangent) and contours of the normalised mean streamwise velocity component U/U_{ref} in the centre-plane of the canyon, for the: (a) NTUA experiment, (b) TU Delft experiment at $Re \approx 60000$.

5.5 Additional Wind Tunnel Tests

In the open jet facility (OJF) of the TU Delft, smaller (by a factor of 3) but geometrically similar models were also used, in order to achieve even lower Reynolds numbers ($Re \leq 30000$) since the lowest achievable wind speed was 3 m/s. These models had been already used in [20].

Co-funded by the European Union

A subsequent experimental campaign has taken place in a smaller open jet facility[7] using the smaller canyon models, under the scope of explaining the differences in flow structure between NTUA and TU Delft. In this case, Stereo-PIV measurements (not shown here) were performed. The results showed that by imposing a favourable pressure gradient in the streamwise direction, as the one that is always present in the NTUA facility due to the enclosed nature of the test section, a similar behaviour is observed between the flow structure captured by the Stereo-PIV measurements (small open jet facility) and the NTUA PTV measurements (enclosed test section).

5.6 Conclusions

A recapitulation of the main findings is the following:

- Scale effects were generally limited for both datasets i.e. the flow structure did not change as Re number increased, but local scale effects were always present, indicating that higher Re may be required to ensure universal Re-independence in the whole examined volume.
- Roof greening has a marginal influence on the flow structure. This was not the case though for the hedge row configuration where the flow behaviour drastically changed e.g. two distinctive vortical structures were present in the centre-plane of the examined canyon.
- The flow exhibited significantly different behaviour between the two facilities. This variation may be attributed to the differing facility types: an open-jet facility at TU Delft and an enclosed, closed-loop wind tunnel at NTUA. Additional measurements revealed that a favourable pressure gradient in the streamwise direction may be the physical explanation behind these differences.

[7] https://www.tudelft.nl/lr/organisatie/afdelingen/flow-physics-and-technology/facilities/low-speed-wind-tunnels/w-tunnel

Co-funded by the European Union

6 Publications

The following publications in national and international conferences and journals have been made from the results of the twin tests.

- A blind test on wind turbine wake modelling based on wind tunnel experiments: Phase I Benchmark case. Pappa, V., Campagnolo, F., Tamaro, S., Mühle, F., Stegmüller, J., Croce, A., Gromke, C., Riziotis, V., Bottasso, C., Sciacchitano, A., Bouris, D., & Manolesos, M. (2024). A blind test on wind turbine wake modelling based on wind tunnel experiments: Phase I - The benchmark case. Journal of Physics: Conference Series, 2767(9), Article 092053. https://doi.org/10.1088/1742-6596/2767/9/092053
- On the three-dimensional coherent structures in the wake of flatback airfoils. Kellaris K, Papadakis G., Manolesos, M., (2024) On the three-dimensional coherent structures in the wake of flatback airfoils, 9th International Colloquium on Bluff Body Aerodynamics and Applications, BBAA IX, Birmingham
- Study of the three-dimensional coherent structures in the wake of flatback airfoils. Kellaris K., Papadakis G. and Manolesos M., (2024, 24-26 September), Study of the three-dimensional coherent structures in the wake of flatback airfoils, 20th EAWE PhD Seminar,Visby, Sweden.
- Δίδυμες Μελέτες, Σε Αεροσήραγγες, Της Ροής Γύρω Από Κτήριο Με Φυτεμένη Όψη Και Δώμα. Βασιλική Παππά, Christof Gromke, Δημήτρης Μπούρης (2024) Δίδυμες Μελέτες, Σε Αεροσήραγγες, Της Ροής Γύρω Από Κτήριο Με Φυτεμένη Όψη Και Δώμα. ΡΟΗ 2024 - 12ο Πανελλήνιο Συνέδριο Φαινόμενα Ροής Ρευστών. Θεσσαλονίκη, 15 – 16 Απριλίου, 2024
- Twin Wind Tunnel tests of a very thick flatback airfoil. Kellaris, K., Calzoni, L., Croce, A., Manolesos, M., (2025) Twin Wind Tunnel tests of a very thick flatback airfoil, Wind Energy Science Conference – EAWE, Nantes, June 2025
- Flow past a building with surface greening: comparison of PIV and LDV in two wind tunnels. Pappa V., Gromke C., Bouris D (2024) Flow past a building with surface greening: comparison of PIV and LDV in two wind tunnels. PHYSMOD 2024 – International Workshop on Physical Modelling of Flow and Dispersion Phenomena. Ecole Centrale de Lyon, Ecully, France – August 28-30, 2024
- A Blind Test on Wind Turbine Wake Modelling: Benchmark Results and Next Steps. Chondromatidis, I., Pappa, V., Dsouza, B. S., Sciacchitano, A., Tamaro, S., Mühle, F. V., Campagnolo, F., Bottasso, C. L. and Manolesos, M., (2025) A Blind Test on Wind Turbine Wake Modelling: Benchmark Results and Next Steps, Wind Energy Science Conference – EAWE, Nantes, June 2025
- Twin wind tunnel tests of flow past a building with openings and façade and rooftop greening. Pappa V., Gromke C., Bouris D. (2024) Twin wind tunnel tests of flow past a building with openings and façade and rooftop greening. 9th Int. Coll. on Bluff Body Aerodynamics and Applications, University of Birmingham, Birmingham, UK, 29th July – 2nd August 2024.
- A blind test on wind turbine wake modelling: Benchmark results and Phase II announcement. Chondromatidis, I., Pappa, V., Dsouza, B. S., Sciacchitano, A., Tamaro, S., Mühle, F. V., Campagnolo, F. and Manolesos, M., (2025) A blind test on wind turbine wake modelling:

Co-funded by the European Union

Benchmark results and Phase II announcement. WAKE Conference 2025, Visby, https://doi.org/10.1088/1742-6596/3016/1/012035

- Μελέτη των δευτερευουσών ασταθειών στον ομόρρου αεροτομής με παχύ χείλος εκφυγής. Κελλάρης, Κ., Παπαδάκης, Γ., Μανωλέσος, Μ., Μελέτη των δευτερευουσών ασταθειών στον ομόρρου αεροτομής με παχύ χείλος εκφυγής, 12ο Πανελλήνιο Συνέδριο Φαινόμενα Ροής Ρευστών ΡΟΗ2024, Θεσσαλονίκη
- The effect of trailing edge vortex generators on flatback airfoils. Kellaris, K., Papadakis, G., Manolesos, M., (2025) The effect of trailing edge vortex generators on flatback airfoils, Wind Energy Science Conference – EAWE, Nantes, June 2025
- An experimental study on the combination of Helix and steering and their effects on wake behaviour. Mühle, F. V., Tamaro, S., Bartolin, D., Campagnolo, F., Pappa, V., Manolesos, M., Dsouza, B. S., Sciacchitano, A., and Bottasso, C. L., An experimental study on the combination of Helix and steering and their effects on wake behaviour, Wind Energy Science Conference – EAWE, Nantes, June 2025
- Pallas N.-P., Pappa V. and Bouris D. (2025) Ensemble-based data assimilation of PIV data for turbulent flow past a surface-mounted cube. 15th International ERCOFTAC Symposium on Engineering Turbulence Modelling and Measurements (ETMM-15), Dubrovnik, 22-24 September 2025.
- Irrenfried C., Pappa V., Gromke C. and Bouris D. (2025) Introduction of a flow penetration metric for evaluating the impact of building covering vegetation on wind-driven natural ventilation of indoor spaces. 15th International ERCOFTAC Symposium on Engineering Turbulence Modelling and Measurements (ETMM-15), Dubrovnik, 22-24 September 2025.
- Pallas N-P, Dsouza B, Bouris D., Sciacchitano A., Gromke C. (2025) Twin wind tunnel investigation of the scale effects on a street canyon flow. 9th European-African Conference on Wind Engineering (EACWE2025), 16–19 June, Trondheim, Norway
- Dsouza B., Pallas N., Yu W., Bouris D., Gromke C. and Sciacchitano A. (2025) Three-dimensional flow topology and Reynolds number independence in an urban street canyon. 21th International Symposium on Flow Visualization, June 21-25, 2025, Tokyo, Japan
- Pappa V., Gromke C., Bouris D (2024) Flow past a building with surface greening: comparison of PIV and LDV in two wind tunnels . PHYSMOD 2024 – International Workshop on Physical Modelling of Flow and Dispersion Phenomena. Ecole Centrale de Lyon, Ecully, France – August 28-30, 2024
- Pappa V., Gromke C., Bouris D. (2024) Twin wind tunnel tests of flow past a building with openings and façade and rooftop greening. 9th Int. Coll. on Bluff Body Aerodynamics and Applications, University of Birmingham, Birmingham, UK, 29th July – 2nd August 2024.
- Pappa V., Bakolas A., Bouris D., Gromke C. (2025) Effects of façade and rooftop greening on the surface pressure distribution of an isolated cubic building with side wall apertures. Journal of Wind Engineering and Industrial Aerodynamics, Volume 265, 2025.

Co-funded by the European Union

7 References

[1] Pappa, V., Gromke, C., & Bouris, D., 2023b. Twin test 1: Effect of vegetation on urban flows. PIV data from NTUA WT experiment and LDV from KIT WT experiment (1.0.0) [Data set]. Zenodo. DOI: 10.5281/zenodo.10019002

[2] Castro, I. and A. Robins (1977). "The flow around a surface-mounted cube in uniform and turbulent streams." Journal of Fluid Mechanics 79.2, pp. 307–335.

[3] Gromke, C. (2018). "Wind tunnel model of the forest and its Reynolds number sensitivity." In: Journal of Wind Engineering and Industrial Aerodynamics 175, pp. 53–64

[4] Lim, H. C, I. P. Castro, and R. P. Hoxey (2007). "Bluff bodies in deep turbulent boundary layers: Reynolds-number issues.", Journal of Fluid Mechanics 571, pp. 97–118

[5] VDI 3783 Part 12. 2000. Environmental Meteorology Physical Modelling of Flow and Dispersion Processes in the atmospheric boundary layer. Applications of wind tunnels. VDI. Berlin: Beuth Verlag.

[6] Pappa, V., Bakolas A., Bouris D., Gromke C. , (2025). Effects of façade and rooftop greening on the surface pressure distribution of an isolated cubic building with side wall apertures, Journal of Wind Engineering and Industrial Aerodynamics, 265, 106174.

[7] Pappa, V., Pallas N-P, Bouris D. Gromke C., Riziotis V., Manolesos M., Prospathopoulos J., Chasapogiannis P., Kellaris K., Vassilopoulos K., (2023) "Twin Test 1: Effects of Vegetation on Flows in the Urban Environment " Twin Test: Book of Reference, TWEET-IE EU project, www.tweet-ie.eu

[8] Hearst, R. J., Gomit, G. and B. Ganapathisubramani (2016). "Effect of turbulence on the wake of a wall-mounted cube." Journal of Fluid Mechanics 804, pp. 513–530.

[9] Kozmar H. (2021). "Flow, turbulence and surface pressure on a wall-mounted cube in turbulent boundary layers." In: Journal of Wind Engineering and Industrial Aerodynamics 210.

[10] V. Pappa et al., "Twin Tests Book of Reference Twin Test 2: Wake interactions of a cluster of turbines and wake steering techniques," Jul. 2024. Accessed: Jul. 02, 2025. [Online]. Available: http://tweet-ie.eu/dp/results/33-TWEET-IED4.1BookofReference_TWT2_v3.pdf

[11] Pappa, V., Mühle, F., Tamaro, S., Sciacchitano, A., & DSouza, B. (2024). Twin Test 2: Wake interactions of a cluster of turbines and wake steering techniques. Wind tunnel data. (1.0.0) [Data set]. Zenodo. https://doi.org/10.5281/zenodo.14017240

[12] I. Chondromatidis *et al.*, "A blind test on wind turbine wake modelling: Benchmark results and Phase II announcement," *J Phys Conf Ser*, vol. 3016, no. 1, p. 012035, May 2025, doi: 10.1088/1742-6596/3016/1/012035.

Co-funded by the European Union

[13] F. V. Mühle, F. M. Heckmeier, F. Campagnolo, and C. Breitsamter, “Wind tunnel investigations of an individual pitch control strategy for wind farm power optimization,” *Wind Energy Science*, vol. 9, no. 5, pp. 1251–1271, May 2024, doi: 10.5194/wes-9-1251-2024.

[14] C. Wang, F. Campagnolo, H. Canet, D. J. Barreiro, and C. L. Bottasso, “How realistic are the wakes of scaled wind turbine models?,” *Wind Energy Science*, vol. 6, no. 3, pp. 961–981, Jun. 2021, doi: 10.5194/wes-6-961-2021.

[15] J. Baker, E. Mayda, and C. Van Dam, “Experimental and computational analysis of thick flatback wind turbine airfoils,” in 44th AIAA Aerospace Sciences Meeting and Exhibit, Reno, Nevada: American Institute of Aeronautics and Astronautics, Jan. 2006. doi: 10.2514/6.2006-193.

[16] Pallas, N.P., Dsouza, B., Pappa, V., Prospathopoulos, J., Chasapogiannis, P., Gromke, C., Sciacchitano, A., Bouris, D. (2023). Twin Test 4: Scale Effects in Urban Flows, URL: http://www.tweet-ie.eu/dp/results/38-TWEET-IED4.1BookofReference_TWT4.pdf , accessed: 07.08.25.

[17] Pallas, N.-P., Dsouza, B., & Pappa, V. (2025). A TWEET-IE project twin test : Scale effects on the flow in an urban street canyon. PTV data from wind tunnel experiments at NTUA and TU Delft. (1.0.0) [Data set] Zenodo, https://doi.org/10.5281/zenodo.15847723 .

[18] Pappa, V., Bouris, D., Theurer, W., & Gromke, C. (2023). A wind tunnel study of aerodynamic effects of façade and roof greening on air exchange from a cubic building. *Building and Environment*, *231*, 110023.

[19] Schneiders, J. F., Scarano, F., Jux, C., & Sciacchitano, A. (2018). Coaxial volumetric velocimetry. *Measurement Science and Technology*, 29(6), 065201.

[20] Dsouza, B., Sciacchitano, A. & Yu, W. (2024). Reynolds Number Independence In An Urban Street Canyon Using 3D Robotic Particle Tracking Velocimetry. *21st International Symposium on Applications of Laser and Imaging Techniques to Fluid Mechanics*, Lisbon, 08-11 July 2024.

[21] Faleiros, D. E., Tuinstra, M., Sciacchitano, A., & Scarano, F. (2019). Generation and control of helium-filled soap bubbles for PIV. Experiments in Fluids, 60, 1–17.

[22] Kim, D., Kim, M., Saredi, E., Scarano, F., & Kim, K. C. (2020). Robotic PTV study of the flow around automotive side-view mirror models. *Experimental Thermal and Fluid Science*, 119, 110202.

Co-funded by the European Union